ELSEVIER

Optical Materials 19 (2002) 123–128

OPTICAL Materials

www.elsevier.com/locate/optmat

High-energy pulse generation from solid-state ultraviolet lasers using large Ce:fluoride crystals

Zhenlin Liu [a,*], Kiyoshi Shimamura [a], Tsuguo Fukuda [a], Toshimasa Kozeki [b], Yuji Suzuki [b], Nobuhiko Sarukura [b]

[a] *Institute for Materials Research, Tohoku University, 2-1-1 Katahira, Aoba-ku, Sendai, Miyagi 980-8577, Japan*
[b] *Institute for Molecular Science, 38 Nishigonaka, Myodaiji, Okazaki, Aichi 444-8585, Japan*

Abstract

A large Ce^{3+}:$LiCaAlF_6$ (Ce:LiCAF) crystal with 15 mm diameter was grown successfully by the Czochralski method. Owing to its large size, 60 mJ, 289 nm pulses were generated directly from a quasi-coaxially pumped Ce:LiCAF laser. In addition, a new noncollinear Brewster-angle-pumping disk oscillator scheme was demonstrated for further output-energy scaling. An ultraviolet solid-state Ce^{3+}:$LiLuF_4$ (Ce:LLF) laser which was pumped transversely by a KrF excimer laser with the repetition rate of 1 Hz produced a 27 mJ, 309 nm pulse using a large Ce:LLF crystal which was grown by the Czochralski method, and the slope efficiency was approximately 17%. © 2002 Elsevier Science B.V. All rights reserved.

Ce^{3+} ion-doped fluoride crystals including $LiCaAlF_6$ (LiCAF) [1,2], and $LiLuF_4$ (LLF) [3,4] have been identified to be efficient and convenient ultraviolet (UV) solid-state laser media. We have reported efficient UV short-pulse generation and amplification in a compact, all-solid-state Ce:LiCAF master oscillator and power amplifier (MOPA) system up to the 14 mJ energy level with 18% extraction efficiency in the amplifier stage [5]. We have also demonstrated an all-solid-state tunable Ce:LLF laser pumped by the fifth harmonic of an Nd:YAG laser [6]. Due to the limited sizes of the available crystals, it was difficult to obtain high energy outputs directly from Ce:fluoride lasers. In this paper, we present the growth of large Ce:LiCAF and Ce:LLF crystals. We will demonstrate an output energy of 30 mJ from a UV solid-state laser using the large Ce:LiCAF crystal grown by the Czochralski (CZ) method [7]. Then we increase the pumping energy for the Ce:LiCAF laser by using two Nd:YAG lasers, and 60 mJ pulses are generated from the Ce:LiCAF laser. Furthermore, we design a new pumping configuration with pumping at Brewster angles on a disk Ce:LiCAF crystal. This Ce:LiCAF laser with a newly designed, noncollinear Brewster-angle-pumping disk oscillator scheme is introduced to scale the output energy significantly. We also report on the gener-

* Corresponding author. Present address: Hosono Transparent Electro-Active Materials Project, ERATO, Japan Science and Technology Corporation (JST), C-1232, KSP, 3-2-1 Sakato, Takatsu-ku, Kawasaki, Kanagawa-213-0012, Japan. Tel.: +81-44-850-9767; fax: +81-44-819-2205.

E-mail address: z-liu@net.ksp.or.jp (Z. Liu).

0925-3467/02/$ - see front matter
PII: S0925-3467(01)00209-9

ation of a 27 mJ, 309 nm pulse from a Ce:LLF oscillator pumped transversely by a KrF excimer laser using a large Ce:LLF crystal, the highest output reported from a Ce:LLF laser to date.

Ce:LiCAF crystal growth was performed in a Czochralski system with automatic diameter control (ADC). A stoichiometric charge composed of commercially available AlF_3, CaF_2 and LiF, of high purity (>99.99%), was used as starting material. In the first growth we used a Cr:LiCAF seed oriented along the *a*-axis. The charges were loaded in 40×40 mm^2 glassy carbon crucibles. The concentration of Cerium in the starting material ranged from 1 to 2 mol%. In order to eliminate water and/or oxygen from the growth chamber, a vacuum treatment was performed before the growth. After the vacuum treatment, the furnace was flushed with Argon and the material was melted at a temperature of 825 °C. The applied growth rate was 0.7 mm/h and the rotation rate was 13 rpm. To prevent severe cracking of the boules, the furnace was cooled at a rate of 25 °C/h. In this way, a large Ce:LiCAF crystal with 15 mm diameter was grown successfully [7].

A schematic diagram of the Ce:LiCAF laser resonator is shown in Fig. 1. The laser resonator is established by a flat high reflector and a flat output coupler with 30% reflection for 290 nm separated by 10 cm. The large Ce:LiCAF crystal grown by described method above (18 mm in diameter, clear aperture 15 mm, length 10 mm) which is doped with 1.2 mol% Ce^{3+} ions is located between the two cavity mirrors. There is no coating on the parallel end faces of the crystal that are perpendicular to the optical axis of the resonator. The fourth harmonic of a Q-switched Nd:YAG laser is used as the pumping source. Because it is difficult to fabricate an end mirror with high reflection for 290 nm and high transmission for 266 nm pump beams while maintaining a high damage threshold, we chose to pump the Ce:LiCAF crystal in a noncollinear pumping condition. A large beam cross section in the gain medium is necessary for obtaining high-energy output. The horizontally polarized pump beam is focused with a 40-cm focal length lens to produce a 5 mm diameter spot at the surface of the Ce:LiCAF crystal without any damage to the crystal. More than 90% of the incident pump pulse energy is absorbed by the crystal. Fig. 2 presents the obtained output energies at 289 nm as a function of the absorbed 266 nm pump energy. The maximum pulse energy was up to 30.5 mJ at 10 Hz at 289 nm, and the slope efficiency was 39%.

To scale the output energy, we increased the pumping energy by using two Nd:YAG lasers to pump the Ce:LiCAF laser. The laser resonator was established using a flat, high reflector and a flat output coupler with 30% reflection separated by 4 cm as shown in Fig. 3. A large Ce:LiCAF crystal

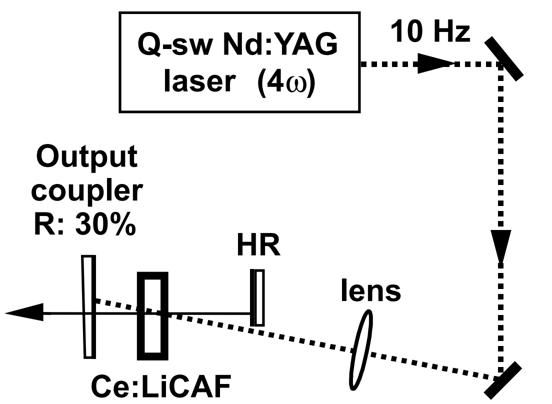

Fig. 1. Experimental setup of the Ce:LiCAF laser oscillator pumped by the fourth harmonic of a Q-switched Nd:YAG laser.

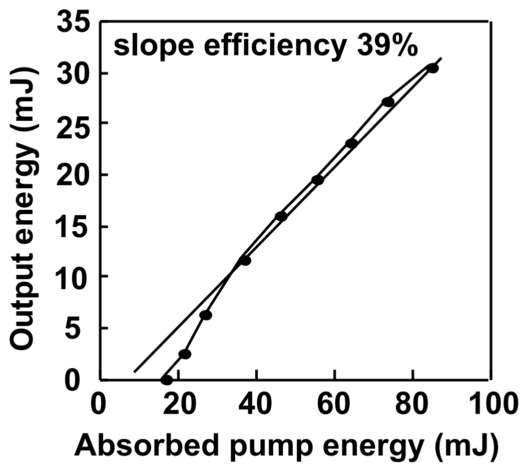

Fig. 2. Laser output energy as a function of absorbed pump energy.

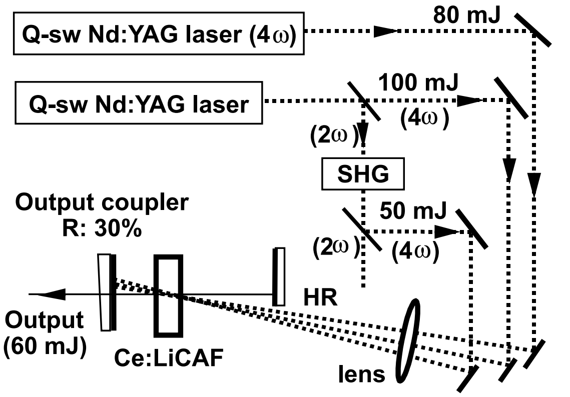

Fig. 3. Experimental setup for high-power Ce:LiCAF laser pumped by the fourth harmonics of two Q-switched Nd:YAG lasers.

(aperture 15 mm, length 10 mm) doped with 1.2 mol% Ce^{3+} ions was located midway between the two cavity end mirrors. The fourth harmonics of two simultaneously Q-switched Nd:YAG lasers were used as the pumping sources. The three pump beams were focused using a 40 cm focal length lens to produce a spot size approximately 6 mm in diameter at the surface of the Ce:LiCAF crystal. With 85% of the total pumping energy of 230 mJ absorbed, the Ce:LiCAF laser produced 60 mJ pulses at a repetition rate of 10 Hz and a wavelength of 289 nm, which is the highest performance reported for a Ce:LiCAF laser until now, as far as we know. No significant power decrease was observed due to the thermal effect for 10 Hz operation compared with 1 Hz operation. LiCAF crystal possesses a negative d*n*/d*t* value (the change of the refractive index with temperature) [8]. Since the negative d*n*/d*t* contribution to the thermal lens tends to cancel the positive effects of thermal expansion, the thermal lensing tends to be very low in LiCAF crystals.

To scale the output energy of a Ce:LiCAF laser, a new pumping scheme permitting efficient, high-energy pumping is necessary. Here, a pumping scheme with pumping at Brewster angles on a disk Ce:LiCAF crystal is proposed. Fig. 4 shows the new pumping scheme schematically. The disk Ce:LiCAF crystal (20 × 20 mm^2 in cross section, 5 mm in length) was placed at the 289 nm wavelength Brewster angle relative to the oscillator axis.

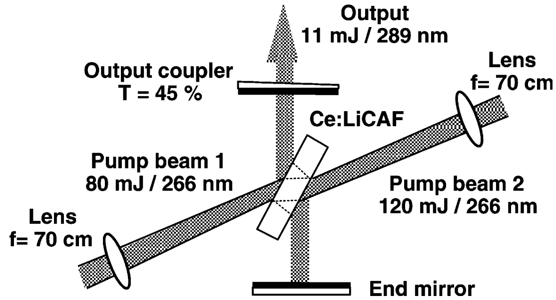

Fig. 4. Experimental setup for disk Ce:LiCAF laser with non-collinear, near-Brewster-angle pumping scheme.

The pumping pulses (the fourth harmonics of two Q-switched Nd:YAG lasers) were directed to the crystal in the direction of the reflection of the Ce:LiCAF laser pulse on the crystal surface. In this case, the pumping pulses at 266 nm wavelength were also near the Brewster angle. Thus, the pumping energy of *p*-polarization pulses could be efficiently coupled into the crystal from the two sides of the crystal without the risk of possible cavity mirror damage as in the collinear pumping scheme [9]. The laser resonator is constructed simply, using a flat, high reflector and a flat output coupler with a transmission of 45% (Fig. 4). The pumping pulses with horizontal polarization from the two Q-switched Nd:YAG lasers operated at 1 Hz were focused softly on the Ce:LiCAF crystal by two 70 cm focal length spherical lenses. The delay between the pumping pulses from the two Nd:YAG lasers was controlled by an electric delay controller. The pumping pulse energies of the two Nd:YAG lasers were 80 and 120 mJ, and approximately 50% of these were absorbed by the Ce:LiCAF crystal. A maximum output energy of 11 mJ was obtained from the Ce:LiCAF laser with Brewster-angle pumping when the pumping pulses from the two Nd:YAG lasers arrived on the crystal simultaneously. Fig. 5 indicates the output-energy dependence on the delay between the two pumping lasers. The upper and lower curves correspond to softer and tighter focusing, respectively. When the relative delay is less than 15 ns, the output pulse has a single pulse shape. When the relative delay becomes larger than 15 ns, the output becomes double pulses for one shot. In the case of higher pulse energy excitation, the temporal trail of the

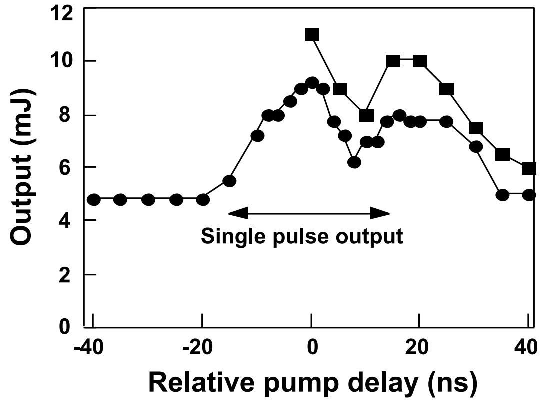

Fig. 5. Output energy dependence on the relative delay of the two pumping Q-switched Nd:YAG lasers. The timing of the 120 mJ pulse was fixed to have a 0 delay, and the relative pump delay position of the 80 mJ pulse was changed from −40 to 40 ns relative to that of the 120 mJ pulse.

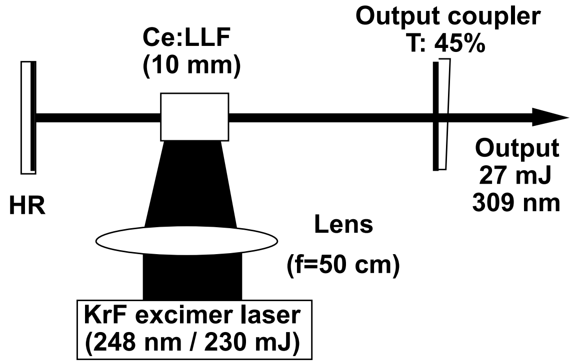

Fig. 6. Experimental setup of the high-power Ce:LLF laser pumped by a randomly polarized KrF excimer laser operated at a repetition of 1 Hz.

output was observed [10]. Such an oscillation trail could be amplified by the secondary pumping pulse. This may be one possible explanation of the bumpy and unsymmetrical dependence of the output on the relative delay of the two pumping pulses. Even though the output is presently not very high, we consider that this noncollinear Brewster-angle-pumping disk oscillator scheme will make it possible to scale the output energy significantly by using larger pumping sources and crystals with higher absorption due to the higher pumping efficiency. The potential advantages of this scheme are the reduced risk of possible mirror damage, ease of pumping beam multiplexing, and better gain profile compared with the side-pumping scheme.

In contrast to Ce:LiCAF crystal (281–314 nm) [11], Ce:LLF crystal has a longer potential tunability in the UV spectral region from 305 to 340 nm, which is attractive for the spectroscopy of wide-band gap semiconductors such as GaN used in blue laser diodes [12]. The Ce:LLF laser resonator is established by using a flat high reflector and a flat output coupler. The length of the laser cavity was 6 cm. The layout is shown schematically in Fig. 6. High-quality, large Ce:LLF crystals ($\varnothing$ 18 mm $\times$ 10 mm in length) were grown successfully at Tohoku University by the Czochralski method [13]. The Ce:LLF sample used here was obtained by cutting the grown Ce:LLF crystal in the middle along its axis (a half-cut cylinder). The side window and two end surfaces were polished. No dielectric coatings were deposited on the polished end surfaces and the side window. The pumping pulses from a randomly polarized KrF excimer laser operated at 1 Hz were focused softly on the side window of the Ce:LLF crystal using a 50-cm-focal-length spherical lens under a normal-incidence side-pumping condition. Because the output pulse of the KrF excimer laser has a rectangular shape, it is not difficult to make a near-line-shape pumping area on the Ce:LLF crystal through a spherical lens. Almost all of the pumping pulse energy (maximum: 230 mJ) was absorbed by the Ce:LLF crystal.

To obtain high output energy from the Ce:LLF laser, we tested some output couplers with different transmissions. The best result was obtained with the coupler with 45% transmission. Fig. 7 shows the input–output dependence curves for the Ce:LLF laser. The maximum output pulse energy reached 27 mJ with the pumping pulse energy of 230 mJ, and the corresponding pumping fluence was approximately 0.6 J/cm^2. This is the highest output pulse energy ever achieved from this laser medium. The free-running Ce:LLF laser operated at the wavelength of 309 nm. The slope efficiency was approximately 17%. To investigate the tuning ability of the Ce:LLF laser, we changed the end mirror of the Ce:LLF laser cavity to a Littrow prism, and the output coupler to one with 10%

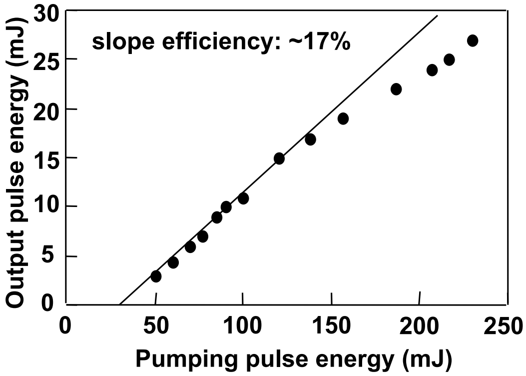

Fig. 7. Input–output dependence curve for the Ce:LLF laser. The maximum output energy reaches 27 mJ at the wavelength of 309 nm.

transmission. First, the tuning was achieved by rotating the prism horizontally. We found that the tuning curve had a gap between the regions around the two fluorescence peaks of Ce:LLF crystal, and that the polarizations of the two regions were perpendicular to each other. To increase the laser efficiency by making use of the Brewster angle condition (there is no reflection for π-polarization light when the incidence angle on the crystal surface is at a Brewster angle), we rotated the prism horizontally and vertically, respectively. When the pumping pulse energy was 100 mJ, a tuning curve for the Ce:LLF laser was obtained, as shown in Fig. 8. The tuning was accomplished from 307.8 to 311.7 nm, and from 323.5 to 326.5 nm with different polarizations. When we attempted to tune the laser longer than 312 nm, the laser operated at two wavelengths that were near 312 and 323 nm. Therefore, under the present condition, the gap of the tuning curve could not be avoided. The phenomena in which the pulses around 309 and 325 nm have different polarizations (perpendicular to each other) can be explained as follows: for the pulses around 309 nm, the effective gain cross section σ_{eg} (gain cross section – ESA cross section; ESA: excited state absorption) for π-polarization light is larger than σ_{eg} for σ-polarization light, while for the pulses around 325 nm, σ_{eg} for π-polarization light is smaller than σ_{eg} for σ-polarization light, or vice versa. Thus, the laser will oscillate in different polarizations at the wavelength regions around 309 and 325 nm. An investigation into the effective gain cross sections for the σ- and π-polarization light of the Ce:LLF crystal is in progress. The tuning result is similar to that in [6], where the Ce:LLF laser was pumped by the fifth harmonic of an Nd:YAG laser. This tuning curve is also quite similar to that of the Ce:YLF laser [14].

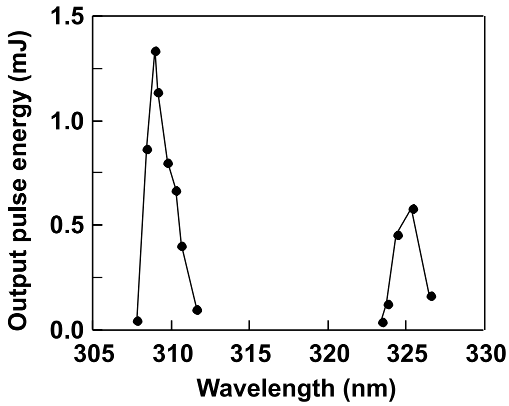

Fig. 8. Tuning curve for the Ce:LLF laser. The pumping energy was 100 mJ. The output coupler has a transmission of 10%.

In summary, large Ce:LiCAF crystals with 15 mm diameter were successfully grown by the Czochralski method. Due to the available large Ce:LiCAF crystal, 60 mJ output energy was obtained from the Ce:LiCAF laser pumped by the fourth harmonics of Q-switched Nd:YAG lasers. This suggests that the Ce:LiCAF is a promising material for high-energy ultraviolet pulse generation combined with high-power, Q-switched Nd:YAG lasers. A very promising pumping scheme with pumping beams at the Brewster angle on the laser crystal surfaces was designed and applied to a Ce:LiCAF laser. In this manner, we demonstrated the very easy and efficient generation of high-energy pulses at 289 nm from Ce: LiCAF lasers. This noncollinear Brewster-angle-pumping disk oscillator scheme will be applicable to many other laser media. A 27 mJ pulse at 309 nm was generated from a UV solid-state Ce:LLF laser using a large Ce:LLF crystal. In this way, we easily and efficiently demonstrated the generation of a high-energy pulse at 309 nm. This is the highest direct output obtained from a Ce:LLF laser reported to date.

References

[1] M.A. Dubinskii, V.V. Semashko, A.K. Naumov, R.Y. Abdulsabirov, S.L. Korableva, in: A.A. PintoT.Y. Fan (Eds.), OSA Proceedings on Advanced Solid-State Lasers, vol. 15, Optical Society of America, Washington, DC, 1993, p. 195.

[2] M.A. Dubinskii, V.V. Semashko, A.K. Naumov, R.Y. Abdulsabirov, S.L. Korableva, J. Mod. Opt. 40 (1993) 1.

[3] M.A. Dubinskii, R.Y. Abdulsabirov, S.L. Korableva, A.K. Naumov, V.V. Semashko, in: International Quantum Electronics Conference, Optical Society of America, Washington, DC, 1992, Paper FrL2.

[4] M.A. Dubinskii, R.Y. Abdulsabirov, S.L. Korableva, A.K. Naumov, V.V. Semashko, Laser Phys. 4 (1994) 480.

[5] N. Sarukura, Z. Liu, H. Ohtake, Y. Segawa, M.A. Dubinskii, R.Y. Abdulsabirov, S.L. Korableva, A.K. Naumov, V.V. Semashko, Opt. Lett. 22 (1997) 994.

[6] N. Sarukura, Z. Liu, S. Izumida, M.A. Dubinskii, R.Y. Abdulsabirov, S.L. Korableva, Appl. Opt. 37 (1998) 6446.

[7] K. Shimamura, N. Mujilatu, K. Nakano, S.L. Baldochi, Z. Liu, H. Ohtake, N. Sarukura, T. Fukuda, J. Crystal Growth 197 (1999) 896.

[8] B.A. Wechsler, D.V. Sumida, in: M.J. Weber (Ed.), CRC Handbook of Laser Science and Technology, Supplement 2: Optical Materials, CRC Press, Boca Raton, FL, 1995, p. 607 (Section 16).

[9] Z. Liu, S. Izumida, H. Ohtake, N. Sarukura, K. Shimamura, N. Mujilatu, S.L. Baldochi, T. Fukuda, Jpn. J. Appl. Phys. 37 (1998) L1318.

[10] N. Sarukura, Z. Liu, Y. Segawa, R.Y. Abdulsabirov, S.L. Korableva, A.K. Naumov, V.V. Semashko, M.A. Dubinskii, Opt. Lett. 20 (1995) 599.

[11] Z. Liu, N. Sarukura, M.A. Dubinskii, R.Y. Abdulsabirov, S.L. Korableva, A.K. Naumov, V.V. Semashko, Jpn. J. Appl. Phys. 37 (1998) L36.

[12] S. Nakamura, M. Senoh, S. Nagahama, N. Iwasa, T. Yamada, T. Matsushita, Y. Sugimoto, H. Kiyoku, Appl. Phys. Lett. 69 (1996) 3034.

[13] I.M. Ranieri, K. Shimamura, K. Nakano, T. Fujita, Z. Liu, N. Sarukura, T. Fukuda, J. Crystal Growth 217 (2000) 151.

[14] P.F. Moulton, Tunable paramagnetic-ion lasers, in: M. Bass M.L. Stitch (Eds.), Laser Handbook, Elsevier, Amsterdam, 1985, p. 284.